Macrocyclization in Cells

DOI: 10.1002/anie.201006140

Controlling Intracellular Macrocyclization for the Imaging of Protease Activity**

*Deju Ye, Gaolin Liang, Man Lung Ma, and Jianghong Rao**

Macrocycles are an important class of molecules for their profound chemical and pharmacological properties derived from the preorganized ring structures.[1–3] They are either isolated from microorganisms or prepared from acyclic precursors through chemical macrocyclization, such as ring-closing olefin metathesis.[4–8] On the other hand, the control of macrocylization to synthesize macrocycles directly from acyclic precursors in living mammalian cells has been little explored. For example, a chemically stable, biologically inactive acyclic precursor (such as **1** in Figure 1) would enter cells and be converted into a macrocycle (such as **3**). Specific cellular processes may be exploited to control the synthesis through regulation of the conversion of the chemically stable precursor into the reactive intermediate (**2** in Figure 1) for subsequent macrocyclization. Because of the unique properties of macrocycles, the conversion from the acyclic into the cyclic form may lead to novel functions and applications for the probing of cellular biochemistry and biology. Herein, we describe an example of the control of macrocyclization in living cells to image local protease activity.

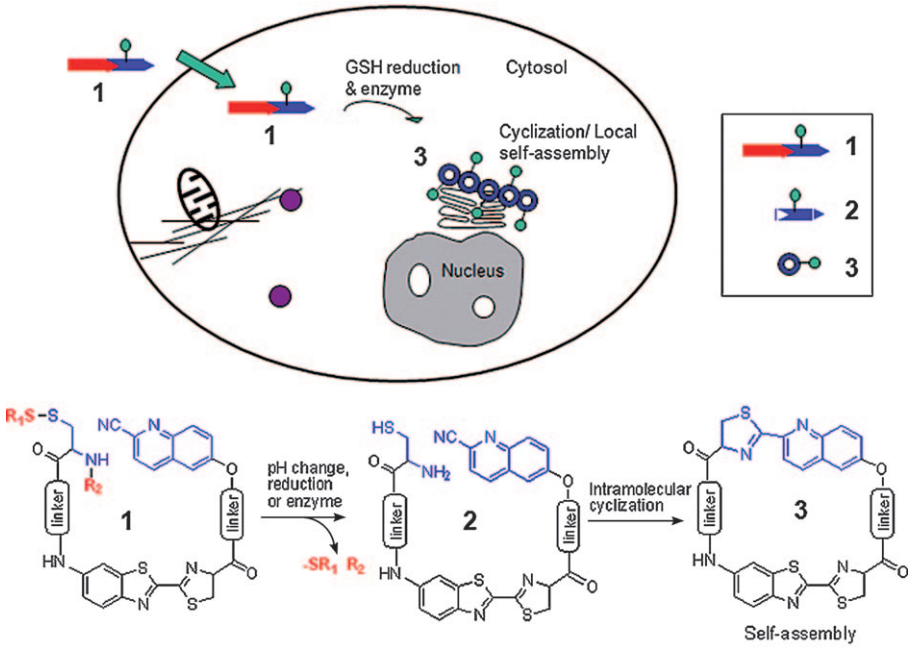

Figure 1. Proposed enzyme-controlled macrocyclization reaction in cells. A cell-permeable probe **1** enters cells and is converted by reduction and/or enzymatic processing into an intermediate **2**, which quickly undergoes intramolecular cyclization to generate the macrocyclic product **3**. The self-assembly of **3** leads to the formation of nanoparticles accumulated locally at or near the enzyme location in cells.

The conceptual design in Figure 1 was demonstrated with an intramolecular macrocyclization system derived from a biocompatible condensation reaction between 2-cyanobenzothiazole (CBT) and free cysteine.[9–12] We have previously shown that this bimolecular condensation reaction can lead to the formation of oligomers in vitro and in cells.[12] For efficient macrocyclization in cells, intermolecular condensation of the acyclic precursors with intracellular endogenous free cysteine should be minimal. We hypothesized that if we used a CBT analogue with significantly reduced reactivity towards cysteine, the acyclic precursor would not react intermolecularly with free cysteine before activation by the target enzyme in cells, but only by an intramolecular cyclization after enzyme-mediated conversion into the reactive intermediate **2**.

To discover such CBT analogues, we screened a series of cyano-substituted aromatic compounds to determine their reaction rates with L-cysteine in phosphate-buffered saline (PBS) in an HPLC assay. A 13-fold decrease in the second-order rate constant was observed for 4-methyl-2-thiazolecarbonitrile, and a more than 480-fold decrease for 2-cyano-6-hydroxyquinoline (CHQ). The other three analogues gave no detectable condensation product on the HPLC column in 5 hours (see Table S1 in the Supporting Information). Aminothiol substrates were also screened for improved activity towards CBT; however, the second-order rate constant of all

[*] Dr. D. Ye, Dr. G. Liang, M. L. Ma, Prof. J. Rao
Molecular Imaging Program at Stanford
Departments of Radiology and Chemistry
Biophysics, Cancer Biology Programs, Stanford University
1201 Welch Road, Stanford, CA 94305-5484 (USA)
Fax: (+1) 650-736-7925
E-mail: jrao@stanford.edu
Homepage: http://raolab.stanford.edu

[**] This research was supported by the Stanford University National Cancer Institute (NCI) Centers of Cancer Nanotechnology Excellence (1U54A151459-01), the NCI ICMIC@Stanford (1P50A114747-06), and an IDEA award from the Department of Defense Breast Cancer Research Program (W81XWH-09-1-0057).

Supporting information for this article is available on the WWW under http://dx.doi.org/10.1002/anie.201006140.

of the tested analogues was lower than that of free cysteine (see Table S1). Therefore, we selected CHQ and cysteine as the reacting pair for the intramolecular-condensation system.

Three precursors **4a–c** containing CHQ and cysteine moieties (Scheme 1) were synthesized to evaluate this hypothesis. A varying number of glycine residues were

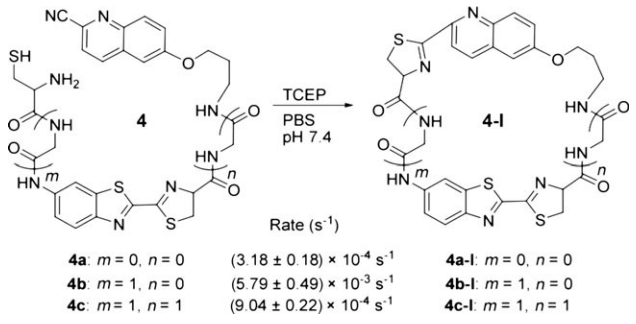

Scheme 1. Intramolecular cyclization of **4a**, **4b**, and **4c** to produce **4a-I**, **4b-I**, and **4c-I**, respectively.

inserted to produce cyclization products with macrocyclic rings of different sizes. All precursors were purified by HPLC and characterized by NMR spectroscopy and MS to confirm their structures (see the Supporting Information).

A similar HPLC assay was employed to measure the reaction rate of the intramolecular cyclization. Upon adjustment of the pH value to 7.4 in the PBS buffer, all three compounds afforded the expected cyclization products, which were cleanly separated by HPLC from the precursors (see Figure S2 in the Supporting Information). The first-order reaction rates are $(3.18 \pm 0.18) \times 10^{-4}\,s^{-1}$ for **4a**, $(5.79 \pm 0.49) \times 10^{-3}\,s^{-1}$ for **4b**, and $(9.04 \pm 0.22) \times 10^{-4}\,s^{-1}$ for **4c**. This result demonstrates that the intramolecular condensation can occur in aqueous solution, and that the reaction rate is affected by the size of the macrocyclic ring formed; **4b** displayed the fastest kinetics with a half-life ($t_{1/2}$) of (119.8 ± 10.2) s.

To further validate that the intramolecular cyclization of CHQ is more favorable than its intermolecular condensation with cysteine, we performed a competition assay with **4c** (5 μM) and varying concentrations of free L-cysteine (0, 5 μM, 500 μM, 5 mM, and 50 mM). The reaction solutions were mixed in the PBS buffer and stirred overnight before analysis by HPLC (see Figure S3). As expected, the amount of product formed by intermolecular condensation slowly increased with the concentration of free L-cysteine; at a concentration of 50 mM of L-cysteine, the ratio of the product of intermolecular condensation to the product of intramolecular macrocyclization was 1:0.76. This result agrees well with the effective molarity of about 48 mM calculated from the ratio of the rate constant of the intermolecular condensation of CHQ and cysteine ($(0.019 \pm 0.001)\,M^{-1}s^{-1}$) to that of the intramolecular cyclization of **4c** ($(9.04 \pm 0.22) \times 10^{-4}\,s^{-1}$). Since the intracellular cysteine concentration is generally around 20–100 μM,[13,14] intermolecular condensation between acyclic precursors or with endogenous free cysteine should be less than 1%, especially for **4b**, which has more than 6.4-fold faster kinetics than **4c** (see Figure S4).

A derivative of **4b** containing a disulfide-protected cysteine residue and an L-lysine residue in place of glycine (**5** in Figure 2a) was prepared to evaluate whether disulfide reduction could trigger intramolecular macrocyclization. Compound **5** was stable at pH 7.4, but upon treatment with the reducing reagent tris(2-carboxyethyl)phosphane (TCEP) at pH 3, it was converted into the reduced form **5-I** (Figure 2b). Subsequent adjustment of the pH value to 7.4 resulted in intramolecular cyclization. Interestingly, in contrast to the reactions of precursors **4a–c**, two product peaks were observed by HPLC analysis with distinct retention times: **5-II-1** and **5-II-2**, which share an identical molecular weight (see Figure S5a). Heteronuclear multiple-bond correlation (HMBC) NMR spectroscopy confirmed that both compounds were macrocyclization products derived from **5** (see Figure S5b). Owing to the presence of L-lysine, they are probably diastereoisomers that arise from two different ring-closing orientations (see Figure S6).

Interestingly, UV/Vis spectroscopy and dynamic light scattering (DLS) revealed that the macrocyclic products derived from **5** could further assemble into nanoparticles, as observed with cyclic oligomers in our previous study.[12] Upon the reduction of **5** with TCEP, the spectrum showed significantly increased broad scattering around 500–700 nm because of the reduction-triggered intramolecular cyclization and aggregation (see Figure S7c,e). DLS further confirmed the formation of particles with a mean diameter of 4–5 μm upon the reduction with TCEP (see Figure S7d,f). TEM images of the products derived from **5** revealed that the macrocycles can self-assemble into nanofibers with an average length of 3–5 μm and an average diameter of 10–20 nm (Figure 2c; see also Figure S7g).

When the hydrophobic dye dansyl chloride was conjugated to the L-lysine side chain of **5**, the new derivative **5d** underwent phase transfer from a homogeneous solution to a suspension upon reduction with TCEP (see Figure S8). TEM images of the cyclized products of **5d** showed self-assembled nanoparticles with diameters of 40–60 nm that could further assemble into clusters (see Figure S8e). Fluorescein isothiocyanate (FITC) was similarly conjugated to form derivative **5f**, which displayed the same reduction-induced macrocyclization and self-assembly of nanoparticles in a buffer and in cell lysates as observed for **5** and **5d** (see Figure S9). These results suggest that the modification of the L-lysine side chain has little effect on the intramolecular cyclization reaction. On the other hand, the control compound **5c** with an S-methylated cysteine residue did not form any cyclized products or aggregates upon reduction with TCEP in the phosphate buffer at a concentration of 100 μM (see Figure S10).

We then investigated whether the intramolecular cyclization could occur in cells. We first incubated **5** (200 μM) in lysates of the human breast cancer cell line MDA-MB-468 for 2 hours. HPLC analysis indicated that the same cyclization products formed as those in the buffer. This result suggests that the intramolecular cyclization can take place in a complex cellular environment containing free intracellular

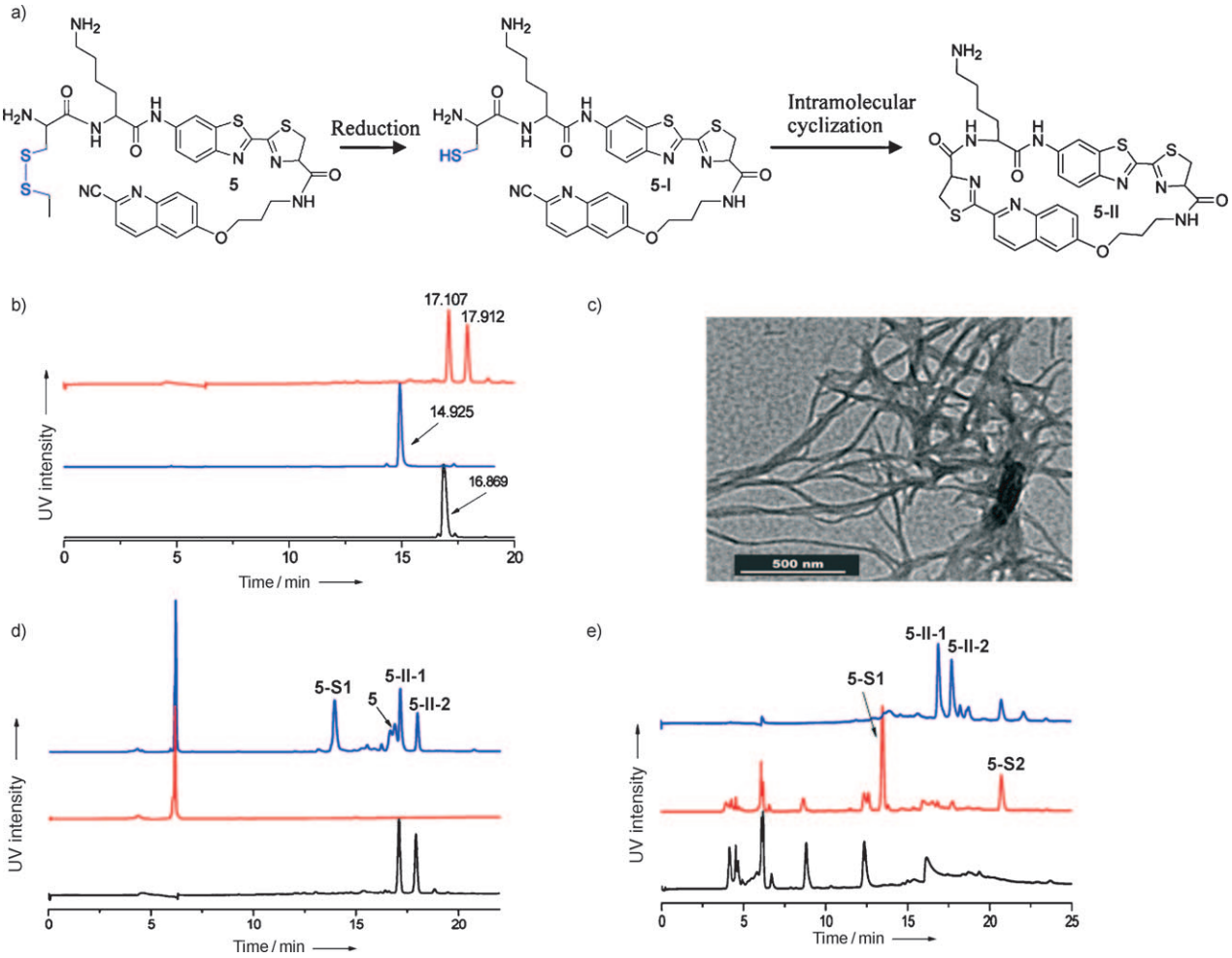

Figure 2. Characterization of the cyclization and nanoassembly induced by chemical or cellular reduction in vitro. a) Proposed two-step reduction-induced cyclization of probe **5**. b) HPLC traces of the cyclization of **5** induced by TCEP reduction. Bottom (black): **5** alone; middle (blue): **5-I** formed by the reduction of **5** (100 μM) by TCEP (200 μM) at pH 3 at room temperature for 20 min; top (red): two cyclized diastereoisomeric products **5-II** formed by the reduction of **5** by TCEP at pH 3 followed by adjustment of the pH value to 7.4. c) TEM image of the products of the TCEP-induced cyclization of **5** (100 μM) in water; 36000× magnification (scale bar: 500 nm). d) HPLC analysis of the intracellular condensation reaction of **5** in cell lysate. Bottom (black): the two cyclized products **5-II-1** and **5-II-2** formed upon the treatment of **5** (200 μM) with TCEP (400 μM) at pH 7.4 at room temperature for 30 min; middle (red): the MDA-MB-468 cell lysate without **5**; top (blue): HPLC trace observed after the incubation of **5** (200 μM) in the MDA-MB-468 cell lysate for 2 h. e) HPLC analysis of the intracellular cyclization reaction of **5** (100 μM) in live cells. Bottom (black): culture medium alone (Dulbecco modified Eagle medium, DMEM); middle (red): the collected medium after the incubation of **5** for 8 h in live MDA-MB-468 cells; top (blue): the lysate of MDA-MB-468 cells incubated with **5** for 8 h.

cysteine. Notably, a side product of **5** with its cysteine residue removed was observed (Figure 2d); this compound, **5-S1**, was presumably formed by proteolytic hydrolysis. Similar results were obtained with HeLa cell lysates (see Figure S11).

We next incubated **5** with live MDA-MB-468 cells for 8 hours and analyzed the cell lysates and culture medium by HPLC and MS spectrometry (Figure 2e). Both intramolecular cyclization products, **5-II-1** and **5-II-2**, were detected in the cell lysates but not in the culture medium, which indicates that the intramolecular cyclization can proceed in live cells, and that the formed macrocycles are retained inside cells. The side product observed in the incubation experiment in cell lysates was also found in the cell medium. An additional side product, **5-S2**, present in the cell medium resulted from the further hydrolysis of **5-S1** and removal of its lysine residue (see Figure S11). Both side products appeared to leak out of cells. When a D-cysteine residue replaced the L-cysteine residue in **5**, neither side product was observed by HPLC (see Figure S12).

The control compound **5c**, on the other hand, did not produce any cyclization products after similar incubation with the MDA-MB-468 cell lysates for 2 hours at 200 μM, although the hydrolysis side products were also observed (see Figure S10b). These results together demonstrate that intracellular reduction by glutathione can induce the intramolecular macrocyclization of CHQ–Cys probes.

To apply this novel chemistry to image protease activity, we designed a probe **6**, which is a conjugate of **5f** with the peptide substrate of the trans-Golgi protease furin (RVRR; Figure 3a).[15] Furin is a convertase that plays crucial roles in development, homeostasis, and diseases ranging from anthrax and Ebola fever to Alzheimer's disease and cancer.[16–19] As

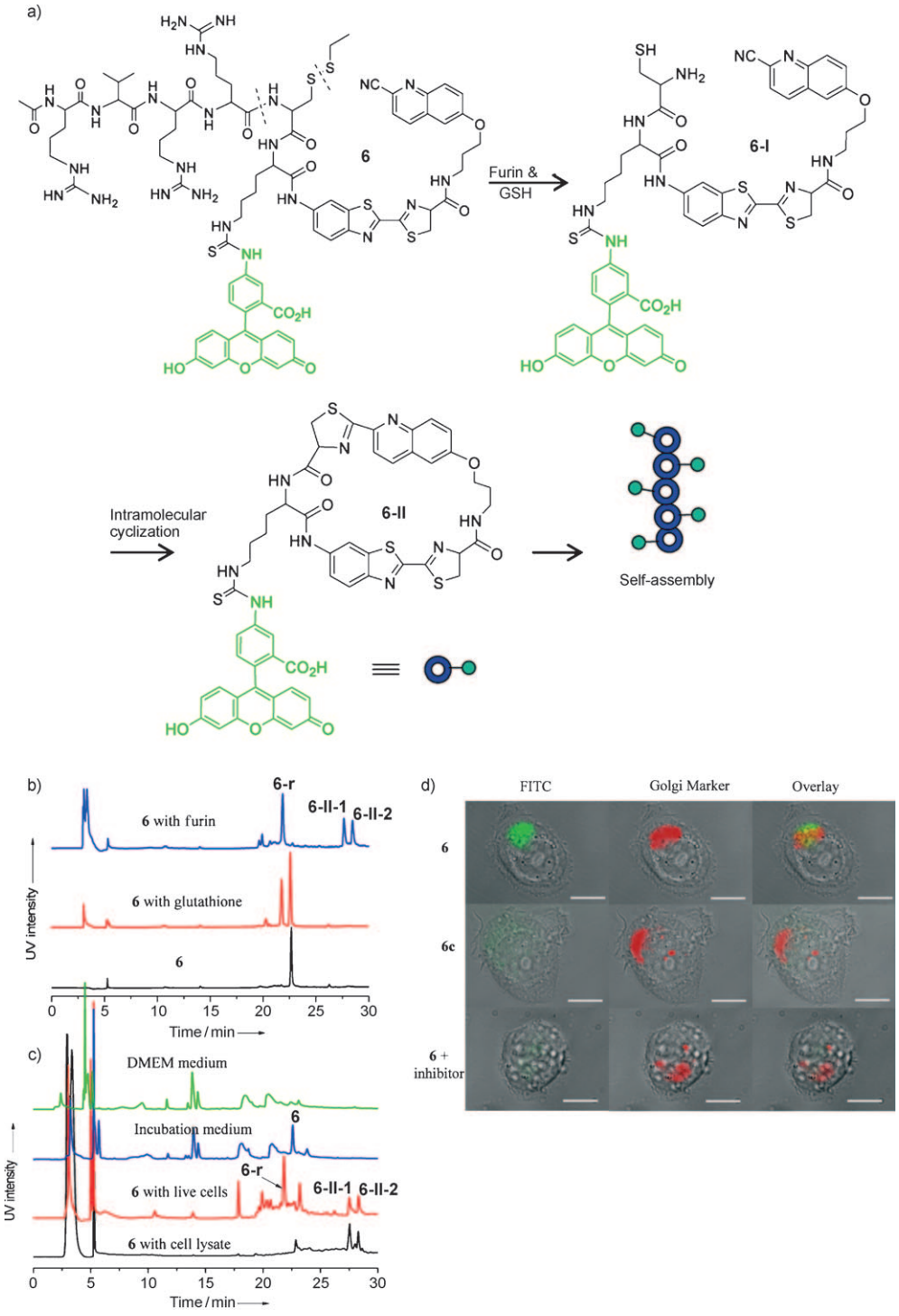

Figure 3. Furin-triggered cyclization in vitro and in live cells. a) Proposed furin-triggered cyclization of probe **6** in cells. Glutathione reduction and furin hydrolysis generate **6-I**. The intracellular cyclization of **6-I** gives **6-II**, which subsequently self-assembles into nanoparticles. b) HPLC traces of **6** (5 μM) in water (bottom, black), after incubation with glutathione (100 μM) for 2 h at 30 °C (middle, red), and after incubation with furin (100 pmol U^{-1}) for 8 h at 30 °C in furin buffer (pH 7.5; top, blue). Compound **6-r** is the disulfide reduced form of **6**. c) HPLC traces of the DMEM medium (green), of the MDA-MB-468 cell lysate after incubation with **6** (20 μM) along with 1 mM $CaCl_2$ at 30 °C overnight (black), of the incubation medium after the incubation of MDA-MB-468 live cells with **6** (20 μM) overnight (blue), and of the cell lysate after the removal of the incubation medium following the incubation of MDA-MB-468 live cells with **6** (20 μM) overnight (red). d) Fluorescence imaging of furin-triggered localized macrocyclization in live cells. The differential interference contrast (DIC) images are overlaid with the fluorescence images; the three images on the right are an overlay of the green and red fluorescence images on top of the DIC images. MDA-MB-468 cells were incubated with probe **6** (1 μM, top), the control probe **6c** (1 μM, middle), or **6** with the furin inhibitor (100 μM, bottom) for 8 h, followed by costaining with a Golgi marker (BODIPY TR C_5-ceramide–BSA complexes). Scale bars: 10 μm.

expected, the treatment of **6** (5 μM) with furin (100 pmol U^{-1}) in vitro generated the two cyclization products **6-II-1** and **6-II-2** as diastereoisomers (Figure 3b). Only the reduced form of **6**, not **6-I**, was observed by HPLC, which suggests that furin cleavage is the rate-limiting step of the multiple-step process. Similarly, overnight incubation of **6** with MDA-MB-468 cell lysates or live cells produced the macrocycles **6-II**, as revealed by the HPLC assay (Figure 3c). No cyclization products were detected by HPLC in the medium used for the incubation of live cells, which confirms that the formed macrocycles are trapped inside cells. This result is consistent with the observed nanoparticle formation after the macrocyclization of **5f** (see Figure S9).

MDA-MB-468 cells were then incubated with **6** (1 μM) for 8 h, followed by costaining with a Golgi marker (fluorescent BODIPY TR C_5-ceramide–BSA complexes; BODIPY = boron dipyrromethene, BSA = bovine serum albumin) and imaging under a fluorescence microscope. A good overlap of green (from the assembled macrocycles) and red fluorescence (from the Golgi marker) was observed. This result supports the hypothesis that the intramolecular cyclization occurred at or near Golgi bodies in cells (Figure 3d). When we used the control probe **6c** (see Figure S13), which contains an S-methylated cysteine residue and thus cannot undergo macrocyclization after furin cleavage, or when we used a furin inhibitor (decanoyl-RVRR-cmk; cmk = chloromethyl

ketone)[20] together with **6**, we observed no concentrated fluorescence signals but instead weak and uniform green fluorescence, which confirmed that furin was responsible for the localized accumulation of **6** near and at the Golgi bodies (Figure 3d; see also Figure S14). Similar imaging results were observed with **6** in other cell lines (see Figure S15). These results demonstrate that this intramolecular macrocyclization reaction can be applied to image local furin activity in living cells.

In comparison to previously reported CBT and cysteine bimolecular condensation systems, an important advantage of this system is that it is not subject to endogenous cysteine competition owing to the low reactivity of the CHQ moiety toward cysteine. Furthermore, the condensation takes place intramolecularly, and thus is not concentration-dependent, and is kinetically fast. The enzyme cleavage is therefore the rate-limiting step in the formation of the aggregated macrocycles, which results in a better correlation of the aggregation sites with the location of enzyme activity.

In summary, we have described a bioorthogonal intramolecular macrocyclization reaction that can occur highly efficiently in live cells. We have shown that macrocyclic products can be synthesized in cells under the control of a proteolytic enzyme and glutathione reduction to image local proteolytic activity. Other applications may be possible, such as the in situ synthesis of macrocyclic molecules to probe cellular function through receptor binding.[21]

Received: September 30, 2010
Revised: December 27, 2010
Published online: February 14, 2011

Keywords: bioorthogonal reactions · macrocycles · nanoparticles · protease imaging · self-assembly

[1] E. M. Driggers, S. P. Hale, J. Lee, N. K. Terrett, *Nat. Rev. Drug Discovery* **2008**, *7*, 608–624.
[2] J. Taunton, J. L. Collins, S. L. Schreiber, *J. Am. Chem. Soc.* **1996**, *118*, 10412–10422.
[3] D. T. Bong, T. D. Clark, J. R. Granja, M. R. Ghadiri, *Angew. Chem.* **2001**, *113*, 1016–1041; *Angew. Chem. Int. Ed.* **2001**, *40*, 988–1011.
[4] L. A. Wessjohann, E. Ruijter, D. Garcia-Rivera, W. Brandt, *Mol. Diversity* **2005**, *9*, 171–186.
[5] L. A. Wessjohann, E. Ruijter, *Top. Curr. Chem.* **2005**, *243*, 137–184.
[6] A. Gradillas, J. Pérez-Castells, *Angew. Chem.* **2006**, *118*, 6232–6247; *Angew. Chem. Int. Ed.* **2006**, *45*, 6086–6101.
[7] O. David, W. J. N. Meester, H. Bieräugel, H. E. Schoemaker, H. Hiemstra, J. H. van Maarseveen, *Angew. Chem.* **2003**, *115*, 4509–4511; *Angew. Chem. Int. Ed.* **2003**, *42*, 4373–4375.
[8] S. Muthana, H. Yu, H. Cao, J. Cheng, X. Chen, *J. Org. Chem.* **2009**, *74*, 2928–2936.
[9] E. H. White, F. McCapra, G. F. Field, W. D. McElroy, *J. Am. Chem. Soc.* **1961**, *83*, 2402–2403.
[10] K. Okada, H. Iio, I. Kubota, T. Goto, *Tetrahedron Lett.* **1974**, *32*, 2771–2774.
[11] H. Ren, F. Xiao, K. Zhan, Y. P. Young, H. Xie, Z. Xia, J. Rao, *Angew. Chem.* **2009**, *121*, 9838–9842; *Angew. Chem. Int. Ed.* **2009**, *48*, 9658–9662.
[12] G. Liang, H. Ren, J. Rao, *Nat. Chem.* **2010**, *2*, 54–60.
[13] S. Park, J. A. Imlay, *J. Bacteriol.* **2003**, *185*, 1942–1950.
[14] M. H. Stipanuk, J. E. Dominy, J.-I. Lee, R. M. Coloso, *J. Nutr.* **2006**, *136*, 1652S–1659S.
[15] M. Hosaka, M. Nagahama, W. S. Kim, T. Watanabe, K. Hatsuzawa, J. Ikemizu, K. Murakami, K. Nakayama, *J. Biol. Chem.* **1991**, *266*, 12127–12130.
[16] G. Thomas, *Nat. Rev. Mol. Cell Biol.* **2002**, *3*, 753–766.
[17] J. Shapiro, N. Sciaky, J. Lee, H. Bosshart, R. H. Angeletti, J. S. Bonifacino, *J. Histochem. Cytochem.* **1997**, *45*, 3–12.
[18] R. V. Talanian, C. Quinlan, S. Trautz, M. C. Hackett, J. A. Mankovich, D. Banach, T. Ghayur, K. D. Brady, W. W. Wong, *J. Biol. Chem.* **1997**, *272*, 9677–9682.
[19] A. Dragulescu-Andrasi, G. Liang, J. Rao, *Bioconjugate Chem.* **2009**, *20*, 1660–1666.
[20] S. Henrich, A. Cameron, G. P. Bourenkov, R. Kiefersauer, R. Huber, I. Lindberg, W. Bode, M. E. Than, *Nat. Struct. Biol.* **2003**, *10*, 520–526.
[21] Z. Yang, G. Liang, B. Xu, *Acc. Chem. Res.* **2008**, *41*, 315–326.

